The interaction of CK2α and CK2β, the subunits of protein kinase CK2, requires CK2β in a pre-formed conformation and is enthalpically driven

Jennifer Raaf[1], Elena Brunstein[1], Olaf-Georg Issinger[2] and Karsten Niefind[1*]

[1] Universität zu Köln, Department für Chemie, Institut für Biochemie, Zülpicher Straße 47, D-50674 Köln, Germany

[2] Syddansk Universitet, Institut for Biokemi og Molekylær Biologi, Campusvej 55, DK-5230 Odense, Denmark

**Corresponding author*

E-mail: Karsten.Niefind@uni-koeln.de; Tel.: +49 221 4706444; Fax: +49 221 4705092

Running title: Structure of the β subunit of protein kinase CK2

Number of manuscript pages: 24

Number of tables: 1

Number of figures: 2

The text was saved with Word2002 for PC.

Abstract

The protein kinase CK2 (former name: "casein kinase 2") predominantly occurs as a heterotetrameric holoenzyme composed of two catalytic chains (CK2α) and two non-catalytic subunits (CK2β). The CK2β subunits form a stable dimer to which the CK2α monomers are attached independently. In contrast to the cyclins in the case of the cyclin-dependent kinases CK2β is no on-switch of CK2α; rather the formation of the CK2 holoenzyme is accompanied with an overall change of the enzyme's profile including a modulation of the substrate specifity, an increase of the thermostability and an allocation of docking sites for membranes and other proteins. In this study we used C-terminal deletion variants of human CK2α and CK2β that were enzymologically fully competent and in particular able to form a heterotetrameric holoenzyme. With differential scanning calorimetry (DSC) we confirmed the strong thermostabilization effect of CK2α on CK2β with an upshift of the CK2α melting temperature of more than nine degrees. Using isothermal titration calorimetry (ITC) we measured a dissociation constant of 12.6 nM. This high affinity between CK2α and CK2β is mainly caused by enthalpic rather than entropic contributions. Finally, we determined a crystal structure of the CK2β construct to 2.8 Å resolution and revealed by structural comparisons with the CK2 holoenzyme structure that the CK2β conformation is largely conserved upon association with CK2α whereas the latter undergoes significant structural adaptions of its backbone.

Keywords

protein kinase CK2; casein kinase 2; catalytic subunit CK2α; regulatory subunit CK2β; x-ray crystallography; isothermal titration and differential scanning calorimetry; thermo-stabilization of CK2α by CK2β; binding affinity between CK2α and CK2β

Protein-protein interactions are fundamental for protein function. They increasingly attract attention as potential targets for small molecules in chemical biology and pharmaceutical chemistry (Wells and McClendon 2007), as subjects for bioinformatic and statistical analyses (Jones and Thornton 1996) or as a challenge for theoretical prediction (Lensink et al. 2007).

The Ser/Thr protein kinase CK2 (former name: "casein kinase 2") provides a prime example of a physiologically relevant protein/protein interaction. In vertebrates CK2 predominantly occurs as a heterotetrameric holoenzyme, i.e. as a complex of two catalytic subunits (CK2α) attached to a stable central dimer of two non-catalytic subunits (CK2β) (Niefind et al. 2001). CK2α is a close relative of the cyclin-dependent kinases and the MAP kinases. It is catalytically active already as a monomer, but the association with CK2β significantly changes its enzymological properties, e.g. its substrate specificity (Pinna 2003), its ability to dock to membranes (Sarrouilhe et al. 1998) or even to penetrate them (Rodriguez et al. 2008). Moreover, CK2α independent roles for CK2β have been suggested (Bibby and Litchfield 2005; Bolanos-Garcia et al. 2006). However, the recruitment of CK2α for the CK2 holoenzyme complex is so far the only validated function. Therefore, the lack of the modulatory impact of CK2β on CK2α may be the reason for the non-viability of CK2β knockout mice (Buchou et al. 2003). To test this hypothesis and to reveal more details of the physiological role of the CK2α/CK2β

interaction small molecule antagonists of CK2β are desirable.

First attempts to develop such substances have been published recently (Raaf et al. 2008; Laudet et al. 2007). These efforts can be supported by structural and biophysical insights about the CK2α/CK2β interaction. Therefore, we present here the first unbound 3D-structure of a CK2β construct that is fully capable of CK2α recruitment and we quantify its affinity to CK2α thermodynamically. This structure supplements existing structures of unbound human CK2α (Ermakova et al. 2003; Raaf et al. 2008; Niefind et al. 2007) and of the "bound case", i.e. the human CK2 holoenzyme (Niefind et al. 2001); thus, it allows a comprehensive view on the conformational changes that occur at the CK2α/CK2β interface upon association.

Results and Discussion

Thermodynamic background

For our analysis we used *hs*CK2β$^{1-193}$, a C-terminally truncated mutant of human CK2β, in order to avoid aggregation problems as reported for the 215 amino acids long wildtype protein (Chantalat et al. 1999b). *Hs*CK2β$^{1-193}$ was among a set of 21 CK2β mutants characterized by Boldyreff et al. (1993). This study demonstrated that the ability of CK2β to bind CK2α critically depends on the C-terminal segment: while *hs*CK2β$^{1-180}$ retained this competence only to a significantly reduced amount, *hs*CK2β$^{1-193}$ was the shortest construct to be similarly

functional as the wildtype. In other words: the CK2β segment from Asn181 to His193 is a key region for the formation of the CK2 holoenzyme.

We confirmed these results as far as they refer to *hs*CK2β$^{1-193}$ with micro-calorimetric methods. First we used differential scanning calorimetry (DSC) to determine the melting temperatures of *hs*CK2β$^{1-193}$, of *hs*CK2α$^{1-335}$ – a fully active C-terminal deletion mutant of human CK2α (Ermakova et al., 2003) – and of a tetrameric complex of both. The resulting temperature scans (Fig. 1A) demonstrate that the melting point of *hs*CK2β$^{1-193}$ changes only marginally by complex formation while that of *hs*CK2α$^{1-335}$ increases from 45.6 °C to 54.7 °C. This strong thermostabilizing impact of *hs*CK2β$^{1-193}$ on *hs*CK2α$^{1-335}$ is fully consistent with former results obtained with the wildtype proteins using circular dicroism spectroscopy (Issinger et al. 1991) and it demonstrates a high affinity between both proteins.

To quantify this affinity we used isothermal titration calorimetry (ITC) (Fig. 1B). Assuming that a *hs*CK2β$^{1-193}$ dimer possesses two equivalent binding sites for *hs*CK2α$^{1-335}$ we determined a dissociation constant of 12.6 nM at 35 °C. This value falls in a range typically reported for transient heterocomplexes (Nooren and Thornton 2003). It is in the same order of magnitude as the K_D value of 5.4 nM measured for the interaction of full-length CK2β with a CK2α/gluthation-S-transferase fusion protein using surface plasmon resonance

(Martel et al. 2002). This equivalence demonstrates that the final 22 amino acids of human CK2β contribute only marginally to the affinity to CK2α.

Remarkably the association of *hs*CK2α$^{1-335}$ and *hs*CK2β$^{1-193}$ is strongly exothermic. The standard free enthalpy ΔG° for the complex formation amounts to -46.6 kJ/mole and stems exclusively from the enthalpic term (ΔH° = -49.0 kJ/mole) while the entropic contribution (-T*ΔS° = +2.4 kJ/mole) slightly disfavours the binding (Fig. 1B). This result is surprising since according to the CK2 holoenzyme structure (Niefind et al. 2001) the critical patch on the CK2α surface – which is located at the outer surface of the β-sheet typical for the N-terminal domain of eukaryotic protein kinases (indicated in Fig. 2A) – is characterized by a cluster of hydrophobic side chains (Fig. 1C). Therefore, one would expect the formation of hydrophobic interactions between the subunits, a release of ordered water molecules and correspondingly a significantly positive entropic term.

A structural comparison of bound and unbound human CK2α suggests a possible explanation of this paradox. In all unbound structures (Ermakova et al. 2003; Raaf et al. 2008; Niefind et al. 2007) the just mentioned surface patch is not directly accessible for CK2β; rather the neighbouring β4β5-loop occurs in a closed and CK2β incompatible conformation (see two representative examples in Fig. 1C). In this state the hydrophobic patch is reduced to a cavity that at best can harbour flat-shaped small molecules (Raaf et al. 2008). As a

consequence unbound human CK2α cannot release a major amount of ordered water molecules during CK2β association.

Only when CK2β binds, the β4β5-loop adopts an open conformation as it is found in the case of human CK2α so far exclusively in both CK2α chains of the CK2 holoenzyme (Niefind et al. 2001) (Fig. 1C). Possibly this open state of human CK2α is energetically more relaxed than the unbound one with the closed β4β5-loop, meaning that the conformational change of CK2α is a potential source of the heat released upon complex formation (Fig. 1B). This notion is currently speculative but it fits conspicuously to the observation that CK2α from *Zea mays* has an open β4β5-loop in nearly all of its crystal structures (Niefind et al. 1998) and simultaneously a significantly higher tendency to exist *in vivo* in a monomeric (unbound) state than its orthologs from higher animals (Dobrowolska et al. 1992). Further structures together with site-directed mutagenesis and ITC data are required to decide whether the β4β5-loop really plays a key role in the context of the CK2 holoenzyme formation.

Crystal structure of hsCK2β$^{1-193}$

Does CK2β – similar to CK2α – change its conformation at the interface region upon CK2 holoenzyme formation? So far this question could not be answered since for CK2β no true unbound case structure existed. Rather the only available structures of free CK2β dimers (Chantalat et al. 1999a; Bertrand et al. 2004) were obtained with C-terminal deletion mutants without

the aforementioned key region from Asn181 to His193 so that they miss the ability to form a CK2 holoenzyme. To close this gap we crystallized *hs*CK2β$^{1-193}$ and determined its structure to 2.8 A resolution (Tab. 1).

The asymmetric unit of the crystals contains two *hs*CK2β$^{1-193}$ chains that are arranged as a dimer via a zinc-stabilized interface as described for the first time for human CK2β$^{1-182}$ (Chantalat et al. 1999a) (Fig. 2A). Similar to previously published CK2β structures (Chantalat et al. 1999a; Bertrand et al. 2004) the N-terminal segment (residues Met1 to Glu5) and parts of the so-called "acidic loop" (Fig. 2A; residues Glu60 to Asp64) are flexible and undefined by electron density.

Like CK2α-bound CK2β within the CK2 holoenzyme (Niefind et al. 2001), each CK2β monomer consists of a "CK2β body" (Glu6-Ala180) composed of two folding domains and a "CK2β tail" (remaining C-terminal segment) (Fig. 2A). This tail is well defined by electron density up to the C-terminus of the construct (His193; Fig. 2B). The CK2β tail of each monomer makes no contact to its own CK2β body; rather it crosses the dimer interface and is closely attached to the body of the second chain (Fig. 2A). Together with helix αF (and some smaller parts) of that body it forms the surface patch that can recruit a CK2α chain (Fig. 2A).

A remarkable detail of the *hs*CK2β$^{1-193}$ structure are two sulfate ions bound at the so-called juxta-dimer interface region (Fig. 2A) whose function as a preferred anchor for several other proteins has been predicted bioinformatically (Bolanos-Garcia et

al. 2006). Conspicuously the CK2β dimer within the CK2 holoenzyme structure (Niefind et al. 2001) contains phosphate ions at very similar locations (Fig. 2C). Finally in the CK2β$^{2-182}$ structure published by Bertrand et al. (2004) one of a total of four CK2β$^{2-182}$ dimers per asymmetric unit uses the equivalent positively charged surface patch to coordinate acidic side chains from a crystallographic neighbour (Fig. 2C). This coincidence reveals an anion binding capability of the juxta-dimer interface region that may in fact be utilized by some of the many interaction partners of CK2β (Bibby and Litchfield 2005).

The CK2β conformation is pre-formed for CK2 holoenzyme formation

To check the adaptability of CK2β at the interface region to CK2α we fitted the *hs*CK2β$^{1-193}$ dimer structure on the CK2β dimer of the CK2 holoenzyme. For this purpose we used the LSQ_improve subroutine of the program O (Jones et al. 1993) which optimizes an initial least-squares fit of equivalent C_α-atoms by iterative inclusion of more residues. The result of this fit was an RMS deviation of 1.1 Å for 361 C_α atoms which are 98.6 % of the ordered residues. The only deviations occur in the flexible acidic loop regions while the tail zones from Asn181 to His193 match well to each other as well as the helices αF which also contribute to CK2α binding.

These results together with the structural overlay in Fig. 2B demonstrate the pre-formed character of the CK2β dimers which contrasts strongly with the aforementioned adaptability of CK2α in the contact region (Fig. 1C). At least up to Ile192 (Fig. 2B)

no significant backbone adaptations occur in CK2β as a consequence of or as a condition for CK2α binding. Like in the CK2β dimer of the holoenzyme the final section of *hs*CK2β$^{1-193}$ forms a small two-stranded antiparallel β-sheet (β-strands 4 and 5) with Tyr188 at the tip of the connecting loop (Fig. 2A/B); however, due to the higher resolution the β-strand geometry is better defined here than in the CK2 holoenzyme structure.

The only distinct conformational changes in that region refer to the C-terminal His193 and to the side chain of Phe190 (Fig. 2B). In the case of His193 this is probably a crystal packing artefact since this residue additionally has different (but well defined) conformations in the two *hs*CK2β$^{1-193}$ monomers. Phe190, however, is known as one of the "hot spots" of the CK2α/CK2β interaction from the CK2 holoenzyme structure (Niefind et al. 2001) and from a recent kinetic and site-directed mutagenesis study (Laudet et al. 2007). This crucial role of Phe190 fits nicely to the change of its side chain rotamere after CK2α attachment illustrated in Fig. 2B.

Taken together, while CK2α undergoes large conformational changes in the contact region upon docking, the critical part of CK2β is pre-formed. The reduced adaptability of CK2β ensures specificity of its interactions with CK2α and possibly a few other protein kinases (Bibby and Litchfield 2005); moreover it increases the prospects of theoretical docking calculations with the *hs*CK2β$^{1-193}$ structure and the chance to develop CK2β antagonists of high selectivity.

Materials and Methods

Protein expression and purification

*Hs*CK2α^{1-335} and *hs*CK2β^{1-193} were expressed recombinantly in *Escherichia coli* BL21(DE3) cells. To generate the CK2 holoenzyme, mixed lysates of the bacterial cells containing the expressed *hs*CK2α^{1-335} and *hs*CK2β^{1-193} proteins were incubated overnight at 4°C. The three proteins - *hs*CK2α^{1-335}, *hs*CK2β^{1-193} and the holoenyzme (*hs*CK2α^{1-335})$_2$(*hs*CK2β^{1-193})$_2$ - were purified with a two-step chromatographic procedure. The first purification step in all three cases was a phosphocellulose chromatography. The column was equilibrated with 300 mM NaCl, 25 mM Tris/HCl, pH 8.5. After protein application and washing a gradient elution was performed using 1 M NaCl, 25 mM Tris/HCl, pH 8.5, as high-salt component. The second step for *hs*CK2β^{1-193} was an anion exchange chromatography with a HiTrap Sepharose Q column (GE HealthCare). The equilibration and low-salt solution of the gradient was 150 mM NaCl, 25 mM Tris/HCl, pH 8.5, and the high-salt component was again 1 M NaCl, 25 mM Tris/HCl, pH 8.5. For *hs*CK2α^{1-335} and the holoenzyme the second purification step was affinity chromatography with a HiTrap Heparin HP column (GE HealthCare). The equilibration and low-salt solution of the gradient was 400 mM NaCl, 25 mM Tris/HCl, pH 8.5, and the high-salt component was 1 M NaCl, 25 mM Tris/HCl, pH 8.5. Finally the proteins were concentrated and rebuffered in 500 mM NaCl, 25 mM Tris/HCl, pH 8.5, by ultrafiltration using AMICON Ultra-15 tubes.

DSC measurements

For DSC data collection we used a VP-DSC differential scanning calorimeter. For each of the three proteins three temperature scans were performed from 20 to 80°C at a scan rate of 25°C/h. The protein concentrations varied between 64 to 96 µM for *hs*CK2α^{1-335}, between 30 and 69 µM for *hs*CK2β^{1-193} and between 30 and 68 µM for the holoenzyme (*hs*CK2α^{1-335})$_2$(*hs*CK2β^{1-193})$_2$. In all cases the protein buffer was 500 mM NaCl, 25 mM Tris/HCl, pH 8.5. Processing of the raw data were performed with the ORIGIN software (version 7), Origin Lab, Northampton, MA, USA.

ITC measurements

All experiments were performed with a Microcal VP-ITC at 35°C. *Hs*CK2β^{1-193} was provided in the sample cell at concentrations between 9 and 23 µM. *Hs*CK2α^{1-335} was regarded as the "ligand"; it was present in the injection syringe at concentrations between 98 and 230 µM. Both proteins were diluted with 500 mM NaCl, 25 mM Tris/HCl, pH 8.5, to the required concentrations and subsequently degassed. Each ITC experiment consisted of 25 injections of 10 µl. The injections were made over a period of 20 s with a 300 s interval between subsequent injections.

The raw ITC data (Fig. 1B, upper panel) were processed with the ORIGIN software (version 7), Origin Lab, Northampton, MA, USA, assuming a binding model of a single set of two equivalent sites (meaning two *hs*CK2α^{1-335} ligands bind to one

*hs*CK2β^{1-193} dimer). The final values (insert of Fig. 1B) are averages of three repetitions.

Crystallization

All crystallization experiments with *hs*CK2β^{1-193} were performed at 20 °C with the vapour diffusion technique. The optimized crystallization condition was 0.17 M ammonium sulfate, 0.085 M sodium cacodylate, pH 6.3, 25.5% w/v PEG 8000 and 15% v/v glycerol for the reservoir. The crystallization drop contained 2 µl of a *hs*CK2β^{1-193} solution (6.6 mg/ml) and 3 µl reservoir. The crystals were directly transferred from the mother liquor to liquid nitrogen for cryo-protection.

Diffraction data collection and structure determination

X-ray diffraction data (Tab. 2) were collected at a temperature of 100 K at the beamline X12 of the EMBL outstation in Hamburg. The wavelength was 0.9 Å. All diffraction data were processed with the HKL package (Otwinowski and Minor 1997). The structure of *hs*CK2β^{1-193} was determined by molecular replacement using MOLREP (CCP4 1994) and refined with REFMAC (CCP4 1994). Manual corrections were performed with O (Jones et al. 1993). The structure was validated with PROCHECK (CCP4 1994).

Availability

The final atomic coordinates and structure factor amplitudes of *hs*CK2β^{1-193} are available from the PDB (accession code 3EED).

Acknowledgments.

We are grateful to the staff of the EMBL outstation in Hamburg, Germany, for assistance with data collection. This work was funded by the Danish Research Council (grant no.21-01-0511) and by the Deutsche Forschungsgemeinschaft (DFG; grant NI 643/1-3).

References

Bertrand, L., Sayed, M.F.R., Pei, X.-Y., Parisini, E., Dhanaraj, V., Bolanos-Garcia, V.M., Allende, J.E., and Blundell, T.L. 2004. Structure of the regulatory subunit of CK2 in the presence of a $p21^{WAF1}$ peptide demonstrates flexibility of the acidic loop. *Acta Crystallogr.* **D60**: 1698-1704.

Bibby, A.C., and Litchfield, D.W. 2005. The multiple personalities of the regulatory subunit of protein kinase CK2: CK2 dependent and CK2 independent roles reveal a secret identity for CK2β. *Int. J. Biol. Sci.* **1**: 67-79.

Bolanos-Garcia, V.M., Fernandez-Recio, J., Allende, J.E., and Blundell, T.L. 2006. Identifying interaction motifs in CK2β - a ubiquitous kinase regulatory subunit. *Trends Biochem. Sci.* **31**: 654-661.

Boldyreff, B., Meggio, F., Pinna, L.A., and Issinger, O.-G. 1993. Reconstitution of normal and hyperactivated forms of casein kinase-2 by variably mutated β-subunits. *Biochemistry* **32**: 12672-12677.

Buchou, T., Vernet, M., Blond, O., Jensen, H.H., Pointu, H., Olsen, B.B., Cochet, C., Issinger, O.-G., and Boldyreff, B. 2003. Disruption of the regulatory β subunit of protein kinase CK2 in mice leads to a cell-autonomous defect and early embryonic lethality. *Mol. Cell. Biol.* **23**: 908-915.

Chantalat, L., Leroy, D., Filhol, O., Nueda, A., Benitez, M.J., Chambaz, E.M., Cochet, C., and Dideberg, O. 1999a.

Crystal structure of the human protein kinase CK2 regulatory subunit reveals its zinc finger-mediated dimerization. *EMBO J.* **18**: 2930–2940.

Chantalat, L., Leroy, D., Filhol, O., Quitaine, N., Chambaz, E.M., Cochet, C., and Dideberg, O. 1999b. Crystallization and preliminary x-ray diffraction analysis of the regulatory subunit of human protein kinase CK2. *Acta Crystallogr.* **D55**: 895-897.

Collaborative Computational Project No. 4, 1994. CCP4 suite: programs for protein crystallography. *Acta Crystallogr.* **D50**: 760-763.

Dobrowolska, G., Meggio, F., Szczegielniak, J., Muszynska, G., and Pinna, L.A. 1992. Purification and characterization of maize seedling casein kinase IIB, a monomeric enzyme immunologically related to the α subunit of animal casein kinase-2. *Eur. J. Biochem.* **204**:299-303.

Ermakova, I., Boldyreff, B., Issinger, O.-G., and Niefind K. 2003. Crystal structure of a C-terminal deletion mutant of human protein kinase CK2 catalytic subunit. *J. Mol. Biol.* **330**: 925-934.

Esnouf, R.M. 1997. An extensively modified version of MolScript that includes greatly enhanced coloring capabilities. *J. Mol. Graph.* **15**: 132-134.

Jones, S., and Thornton, J.M. 1996. Principles of protein-protein interactions. *Proc. Natl. Acad. Sci. U. S. A.* **93**: 13-20.

Jones, T.A., Zou, J.-Y., Cowan, S.W., and Kjeldgaard, M. 1991. Improved methods for building protein models in electron density maps and location of errors in these models. *Acta Crystallogr.* **A47**: 110-119.

Laudet, B., Barette, C., Dulery, V., Renaudet, O., Dumy, P., Metz, A., Prudent, R., Deshiere, A., Dideberg, O., Filhol, O., and Cochet, C. 2007. Structure-based design of small peptide inhibitors of protein kinase CK2 subunit interaction. *Biochem. J.* **408**: 363-373.

Lensink, M.F., Méndez, R. and Wodak, S.J. 2007. Docking and scoring protein complexes: CAPRI 3rd edition. *Proteins* **69**: 704-718.

Martel, V., Filhol, O., Nueda, A., and Cochet, C. 2002. Dynamic localization/association of protein kinase CK2 subunits in living cells: a role in its cellular regulation? *Ann. N. Y. Acad. Sci.* **973**: 272-277.

Merrit, E.A., and Bacon, D.J. 1997. Raster3D: photorealistic molecular graphics. *Methods Enzymol.* **277**: 505-524.

Niefind, K., Guerra, B., Ermakowa, I., and Issinger, O.-G. 2001. Crystal structure of human protein kinase CK2: insights into basic properties of the CK2 holoenzyme. *EMBO J.* **20**: 5320–5331.

Niefind, K., Guerra, B., Pinna, L.A., Issinger, O.-G., and Schomburg, D. 1998. Crystal structure of the catalytic subunit of protein kinase CK2 from *Zea mays* at 2.1 Å resolution. *EMBO J.* **17**: 2451-2462.

Niefind, K., Yde, C.W., Ermakova, I., and Issinger, O.-G. 2007. Evolved to be active: sulfate ions define substrate recognition sites of CK2α and emphasise its exceptional role within the CMGC family of eukaryotic protein kinases. *J. Mol. Biol.* **370**: 427-438.

Nooren, I.M.A., and Thornton, J.M. 2003. Structural characterization and functional significance of transient protein-protein interactions. *J. Mol. Biol.* **325**: 991-1018.

Otwinowski, Z., and Minor, W. 1997. Processing of X-ray diffraction data collected in oscillation mode. *Methods Enzymol.* **276**: 307-326.

Pinna, L.A. 2003. The raison d'être of constitutively active protein kinases: the lesson of CK2. *Acc. Chem. Res.* **36**:378-384.

Raaf, J., Brunstein, E., Issinger, O.-G., and Niefind, K. 2008. The subunit interface of protein kinase CK2 harbors a small molecule binding pocket. *Chem. Biol.* **15**: 111-117.

Rodriguez, F.A., Contreras, C., Bolanos-Garcia, V., and Allende, J.E. 2008. Protein kinase CK2 as an ectokinase: the role of the regulatory CK2β subunit. *Proc. Natl. Acad. Sci. U. S. A.* **105**: 5693-5698.

Sarrouilhe, D., Filhol, O., Leroy, D., Bonello, G., Baudry, M., Chambaz, E.M., and Cochet C. 1998. The tight association of protein kinase CK2 with plasma membranes is mediated by a specific domain of its regulatory β-subunit. *Biochim. Biophys. Acta* **1403**: 199-210.

Schomburg, D., and Reichelt, J. 1988. BRAGI: a comprehensive protein modeling program system. *J. Mol. Graph.* **6**: 161-165.

Wells, J.A., and McClendon, C.L. 2007. Reaching for high-hanging fruit in drug discovery at protein-protein interfaces. *Nature* **450**: 1001-1009.

Figure legends

Fig. 1: Calorimetric and structural analysis of the CK2α/CK2β interaction

A) DSC curves of *hs*CK2α^{1-335} (red), *hs*CK2β^{1-193} (blue) and the corresponding holoenzyme [(*hs*CK2α^{1-335})$_2$(*hs*CK2β^{1-193})$_2$] (black). One representative example out of three repetitions, respectively, is drawn; the indicated melting points are the corresponding average values.

B) ITC profile of the *hs*CK2α^{1-335}/*hs*CK2β^{1-193} interaction. A representative example out of three ITC runs is documentated. The upper half shows the original heat production upon injection and the lower one the integrated and dilution corrected peaks. The final thermodynamic parameters in the insert are average values over three repetitions.

C) The CK2β binding region of human CK2α. The figure is based on the structure of *hs*CK2α^{1-335} in complex with 5,6-dichloro-1-β-D-ribofuranosylbenzimidazole (DRB) (2RKP; Raaf et al. 2008). After structural superimposition the β4β5-loops of *hs*CK2α^{1-335} in complex with sulfate ions (1PVR; Niefind et al. 2007; black colour) and of a *hs*CK2α chain within the CK2 holoenzyme (1JWH; Niefind et al. 2001; blue colour) are drawn. Some hydrophobic side chains of the interface (yellow) and of the tip of the β4β5-loop (grey: closed conformation; blue: open conformation) are added. The figure was prepared with BRAGI (Schomburg and Reichelt 1988).

Fig. 2: Structure of *hs*CK2β^{1-193}

A) Overall ribbon presentation of the *hs*CK2β^{1-193} dimer.

Each *hs*CK2β^{1-193} monomer consists of a body comprising two domains (subunit A: blue/red; subunit B: green/yellow) and a C-terminal tail. The β-sheets of the N-terminal CK2α domains of the CK2 holoenzyme structure (Niefind et al. 2001) were drawn as black C_α-traces after structural superimposition to indicate the location of the CK2α/CK2β interface. Two sulfate ions found at the juxta-dimer interface region are covered with FoFc-omit density (cutoff level 3 σ above the mean). The figure was drawn with BOBSCRIPT (Esnouf 1997) and Raster3D (Merrit and Bacon 1997).

B) Stereo picture of the C-terminal two-stranded β-sheet (β4β5) of a *hs*CK2β^{1-193} monomer.

For reasons of clarity some side chains were left out. The *hs*CK2β^{1-193} structure segment is covered by electron density drawn with a contour level of 1 σ. The purple dotted lines indicate hydrogen bonds; distances are given in Å. For comparison the backbone of the equivalent region of the CK2 holoenzyme together with some side chains are drawn in black colour. The figure was prepared with BOBSCRIPT (Esnouf 1997) and Raster3D (Merrit and Bacon 1997).

C) Stereo picture of the anion binding sites at the juxta-dimer interface region.

The sites are occupied by sulfate ions in the *hs*CK2β^{1-193}

structure, by phosphate ions (black) in the CK2 holoenzyme structure (Niefind et al. 2001) and by negatively charged side chains from a crystallographic neighbour (ball-and-sticks representation of reduced size) in one of four dimers per asymmetric unit of the CK2β^{2-182} structure (Bertrand et al. 2004). The sulfate ions are covered with blue, the protein parts of *hs*CK2β^{1-193} with green pieces of electron density (all taken from the final 2Fo-Fc density map and contoured with a cutoff level of 1 σ). Some hydrogen bonds to the sulfate ions are indicated by dotted lines in magenta colour. The figure was prepared with BOBSCRIPT (Esnouf 1997) and Raster3D (Merrit and Bacon 1997).

Tables

Table 1: Data collection and refinement statistics of the *hs*CK2β^{1-193} crystals

Data collection	
Space group	$P4_12_12$
Cell dimensions	
a, *b*, *c* [Å]	116.46, 116.46, 76.09
α, β, γ[°]	90.0, 90.0, 90.0
Resolution [Å] (highest shell)	29.7 – 2.8 (2.9 – 2.8)
R_{sym} [%] (highest shell)	9.9 (61.8)
$I / \sigma I$ (highest shell)	29.9 (4.6)
Completeness [%] (highest shell)	100.0 (100.0)
Redundancy (highest shell)	13.1 (13.2)
Wilson-plot B-factor [Å^2]	71.0
Refinement	
Resolution [Å]	29.7 – 2.8
No. of reflections	13382
R_{work} / R_{free} [%]	17.2 / 21.5
No. of protomers per AU	2
Missing (disordered) residues	Met1 – Glu5, Glu60 - Asp64
No. of atoms per AU	
Protein	3000
zinc and sulfate ions	17
Water	82
Average B-Factors [Å^2]	
Protein	62.0
zinc and sulfate ions	103.2
Water	45.4
R.m.s. deviations	
bond lengths [Å]	0.011
bond angles [°]	1.123

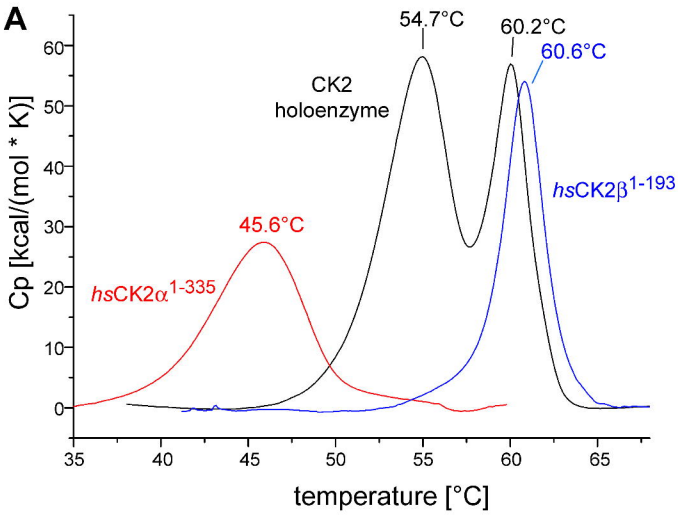
A
54.7°C
60.2°C
60.6°C
CK2
holoenzyme
hsCK2β1-193
45.6°C
hsCK2α1-335
Cp [kcal/(mol * K)]
temperature [°C]

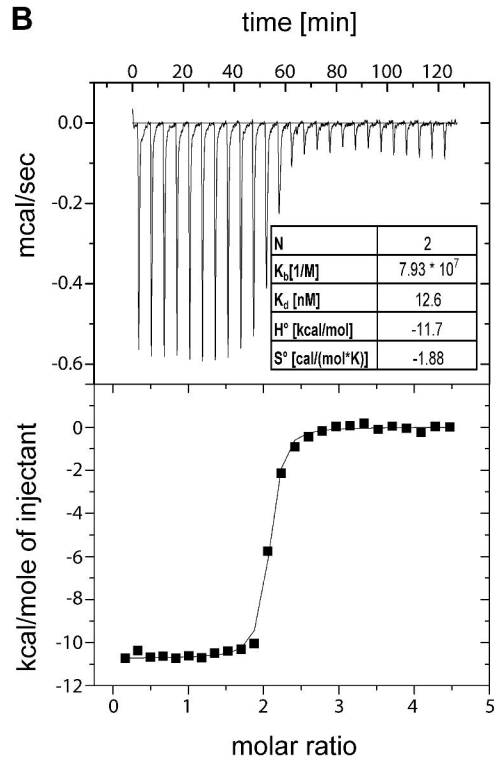
B
time [min]
mcal/sec
N 2
Kb[1/M] 7.93 * 10^7
Kd [nM] 12.6
H° [kcal/mol] -11.7
S° [cal/(mol*K)] -1.88
kcal/mole of injectant
molar ratio

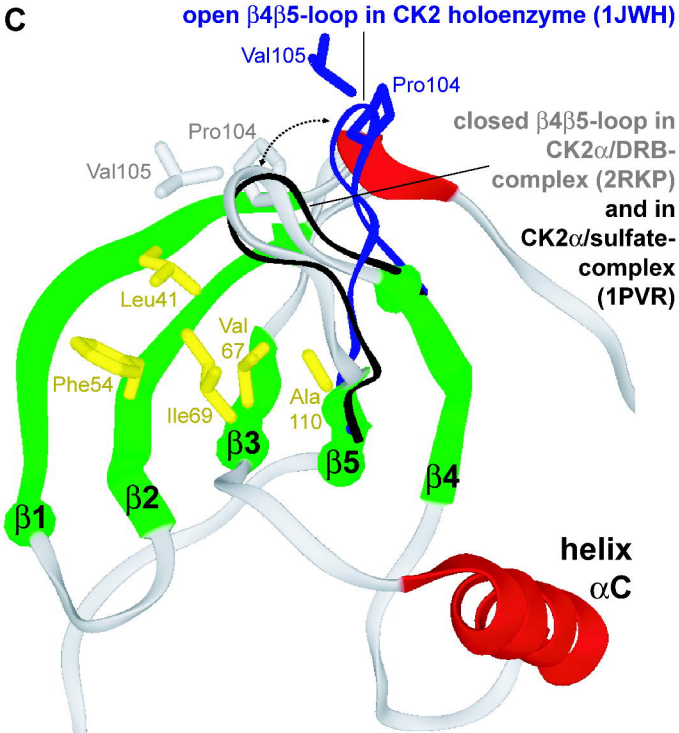
C
open β4β5-loop in CK2 holoenzyme (1JWH)
Val105
Pro104
Pro104
Val105
closed β4β5-loop in CK2α/DRB-complex (2RKP) and in CK2α/sulfate-complex (1PVR)
Leu41
Val 67
Phe54
Ile69
Ala 110
β3
β5
β4
β2
β1
helix αC

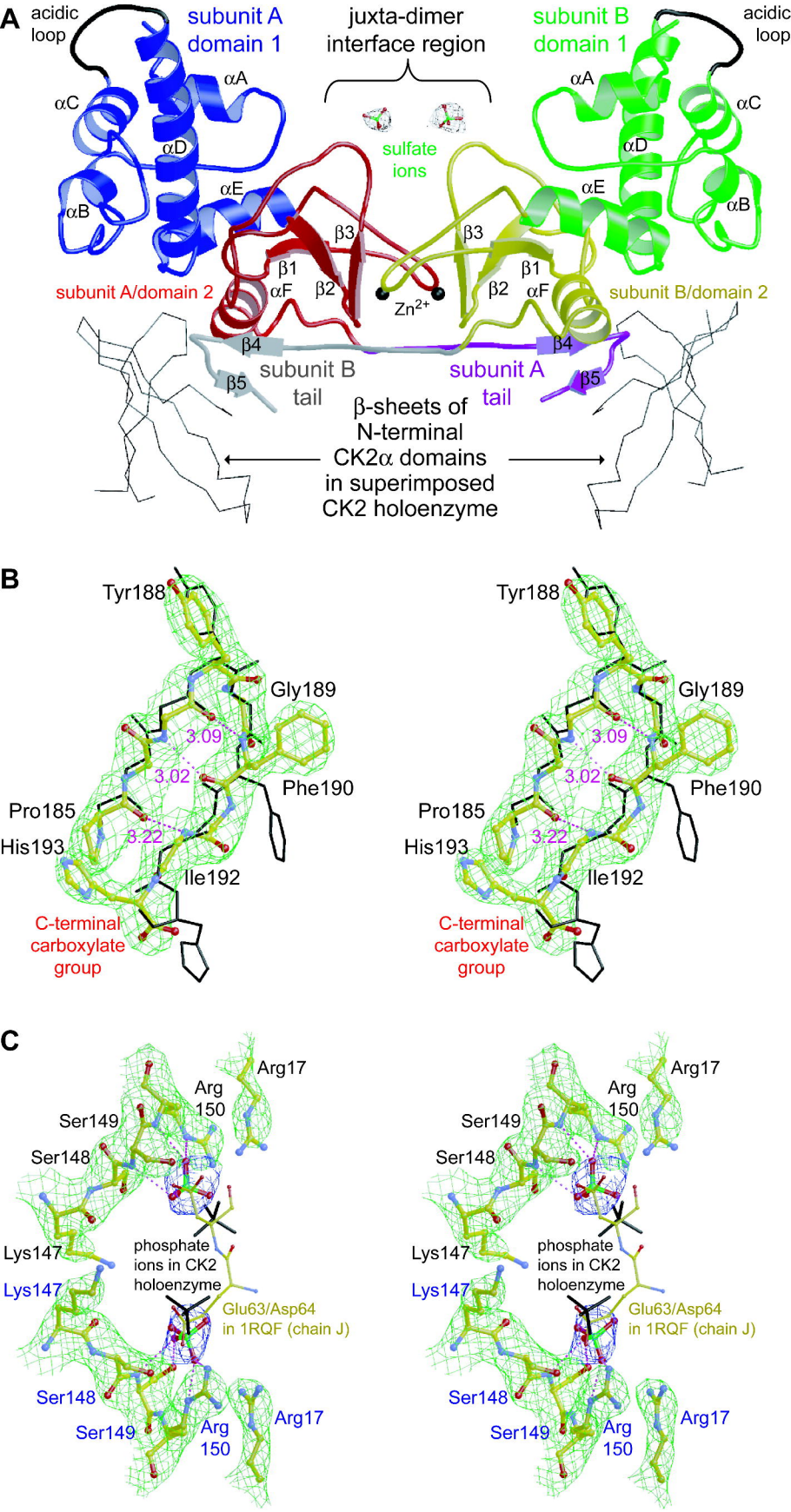
A
acidic loop
subunit A domain 1
juxta-dimer interface region
subunit B domain 1
acidic loop
αA
αC
αD
αE
αB
sulfate ions
β3
β1
αF
β2
Zn2+
subunit A/domain 2
subunit B/domain 2
β4
β5
subunit B tail
subunit A tail
β-sheets of N-terminal CK2α domains in superimposed CK2 holoenzyme
B
Tyr188
Gly189
3.09
3.02
Phe190
Pro185
His193
3.22
Ile192
C-terminal carboxylate group
C
Arg17
Arg 150
Ser149
Ser148
Lys147
phosphate ions in CK2 holoenzyme
Glu63/Asp64 in 1RQF (chain J)